Article

Cell Metabolism

Physiological and Molecular Dissection of Daily Variance in Exercise Capacity

Graphical Abstract

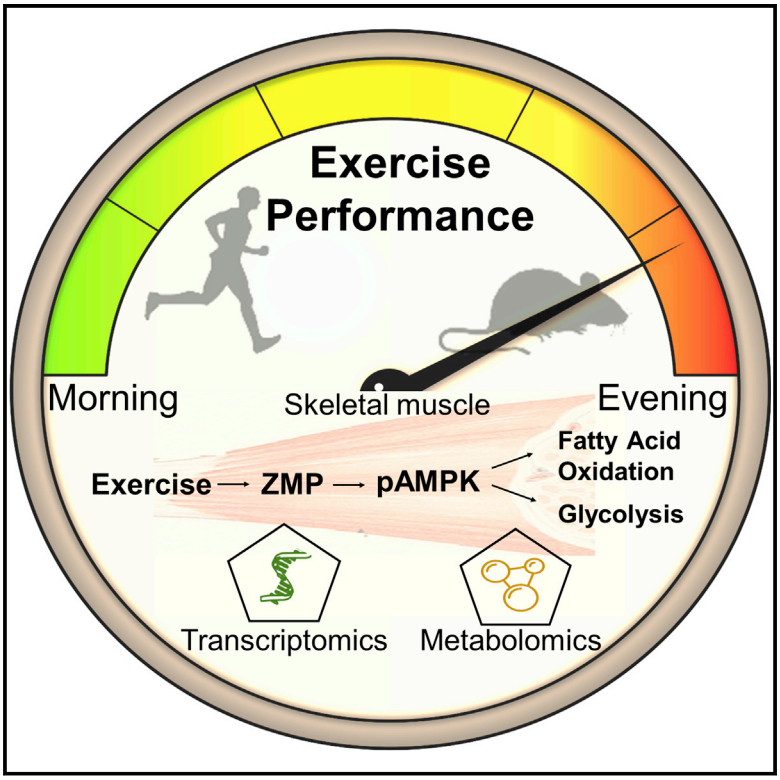

Authors

Saar Ezagouri, Ziv Zwighaft, Jonathan Sobel, ..., Marina Golik, Samuel Verges, Gad Asher

Correspondence

gad.asher@weizmann.ac.il

In Brief

Ezagouri et al. examine the daily variance in exercise capacity in mice and humans. They show that it is affected by exercise intensity and clock proteins and elicits a distinct muscle transcriptomic and metabolic signature. Specifically, they demonstrate that ZMP, an AMPK activator, is induced by exercise in a daytime-dependent manner.

Highlights

- Mice and humans show daily variance in exercise capacity
- Exercise intensity and clock proteins affect daytime variance in exercise capacity
- Exercise elicits distinct daytime muscle transcriptomic and metabolic signature
- ZMP, an AMPK activator, is induced by exercise in a daytime-dependent manner

Ezagouri et al., 2019, Cell Metabolism *30*, 1–14
July 2, 2019
https://doi.org/10.1016/j.cmet.2019.03.012

CellPress

Please cite this article in press as: Ezagouri et al., Physiological and Molecular Dissection of Daily Variance in Exercise Capacity, Cell Metabolism (2019), https://doi.org/10.1016/j.cmet.2019.03.012

Cell Metabolism
Article

Physiological and Molecular Dissection of Daily Variance in Exercise Capacity

Saar Ezagouri,[1,3] Ziv Zwighaft,[1,3] Jonathan Sobel,[1,3] Sébastien Baillieul,[2] Stéphane Doutreleau,[2] Benjamin Ladeuix,[1] Marina Golik,[1] Samuel Verges,[2] and Gad Asher[1,4,*]
[1]Department of Biomolecular Sciences, Weizmann Institute of Science, 7610001 Rehovot, Israel
[2]HP2 Laboratory, Inserm U1042, University Grenoble Alpes, Grenoble, France
[3]These authors contributed equally
[4]Lead Contact
*Correspondence: gad.asher@weizmann.ac.il
https://doi.org/10.1016/j.cmet.2019.03.012

SUMMARY

Physical performance relies on the concerted action of myriad responses, many of which are under circadian clock control. Little is known, however, regarding the time-dependent effect on exercise performance at the molecular level. We found that both mice and humans exhibit daytime variance in exercise capacity between the early and late part of their active phase. The daytime variance in mice was dependent on exercise intensity and relied on the circadian clock proteins PER1/2. High-throughput gene expression and metabolic profiling of skeletal muscle revealed metabolic pathways that are differently activated upon exercise in a daytime-dependent manner. Remarkably, we discovered that ZMP, an endogenous AMPK activator, is induced by exercise in a time-dependent manner to regulate key steps in glycolytic and fatty acid oxidation pathways and potentially enhance exercise capacity. Overall, we propose that time of day is a major modifier of exercise capacity and associated metabolic pathways.

INTRODUCTION

Physical activity is an intricate pleotropic process that relies on the coordinated function of cells, tissues, and organs. Exercise imposes a major challenge to whole-body homeostasis and thus elicits a myriad of adaptive responses at the cellular and systemic levels to redistribute resources and address the increase in muscle energy demands (Egan and Zierath, 2013; Hawley et al., 2014). Nowadays, exercise is widely accepted as a major benefactor for human health and is often recommended for prevention and mitigation of morbidities such as obesity, type 2 diabetes mellitus, and cardiovascular diseases (Cartee et al., 2016; Distefano and Goodpaster, 2018; Fan and Evans, 2017). There is, therefore, a growing interest in deciphering exercise biology, namely identifying molecular events associated with physical activity that affect exercise capacity and carry health benefits (Gabriel and Zierath, 2017).

The physiology and behavior of mammals exhibit daily oscillations that are driven by an endogenous circadian clock (Bass and Lazar, 2016; Bass and Takahashi, 2010; Panda, 2016). The mammalian circadian timing system consists of a central pacemaker in the brain that is entrained by daily light-dark cycles and synchronizes subsidiary oscillators in virtually every cell of the body mostly through rest-activity and feeding-fasting cycles (Dibner et al., 2010; Partch et al., 2014; Reinke and Asher, 2019). The pervasive circadian control of metabolism raises the question of whether exercise performance exhibits daily variance. Hitherto, several human studies supported daily variance in exercise performance (Drust et al., 2005; Küüsmaa et al., 2016; Reilly and Waterhouse, 2009; Thosar et al., 2018). Yet the circadian clock control and the associated time- and exercise-dependent molecular events are relatively unknown. Hence, we hypothesized that studying exercise biology through the prism of time is expected to shed light on molecular mechanisms that are implicated in physical activity and potentially affect exercise capacity.

We characterized herein the daily variance in exercise capacity at the physiological and molecular levels. In essence, we asked the following questions: Is there a daytime difference in

Context and Significance

Exercise is an effective lifestyle intervention for the prevention and mitigation of various diseases. In addition, improvement of exercise performance is of interest for elite and amateur athletes. Therefore, there is growing interest in optimizing the benefits of exercise and its performance. Weizmann Institute researchers investigated whether the time of day and circadian clock affect exercise performance and related metabolic pathways in mice and humans. They found exercise performance is better in the evening than in the morning hours; it relies on the circadian clock and produces a distinct daytime-dependent response in the muscle. These results suggest that timing exercise during the day can affect exercise capacity and be applied to improve exercise performance and potentially optimize health benefits.

exercise capacity? Does it rely on core components of the circadian clock machinery? What are the underlying molecular events? To this end, mice were enrolled in exercise protocols at different times of day. Concurrently, we monitored their exercise capacity and characterized the changes in their skeletal muscle gene expression and metabolic profiles. Furthermore, we corroborated our findings with human studies. Overall, our results suggest that time of day is a central modifier of exercise capacity and related metabolic pathways.

RESULTS

Exercise Capacity Is Daytime Dependent and Clock-Component Regulated

Physical performance relies on the concerted action of myriad responses, many of which are under circadian clock control. This prompted us to test whether exercise capacity differs throughout the day. Specifically, since exercise is typically performed during the active phase, we examined the difference in exercise capacity of wild-type mice between two time points within their active phase, namely 2 h and 10 h within the dark phase (i.e., zeitgeber time [ZT]14 and ZT22, thereby termed Early and Late, respectively). The food consumption and spontaneous locomotor activity of wild-type mice 2 h prior to the exercise tests did not significantly differ between the Early and Late groups (Figure S1A). We tested the treadmill performance of sedentary wild-type mice under 3 different protocols: high, moderate, and low intensities that generally correspond to 100%, 55%, and 45% of their maximal aerobic capacity, respectively (Figure 1A). Sedentary mice slightly outperformed the high-intensity exercise protocol at the early part of their active phase (Figure 1B). By contrast, in the moderate- (Figure 1C) and low-intensity (Figure 1D) protocols, the Late group performed substantially better than the Early group, running for a longer time and maintaining higher blood glucose levels (i.e., above 70 mmol/dL) for a longer duration. Hence, we concluded that exercise capacity exhibits daily variance that is dependent on exercise intensity.

In view of the pervasive clock control of metabolism and physiology (Asher and Sassone-Corsi, 2015; Panda, 2016; Reinke and Asher, 2019), we examined whether the variance in exercise capacity relies on a functional circadian clock. To this end, we tested the clock mutant *Per1/2*$^{-/-}$ mice, which exhibit arrhythmic behavior in constant darkness and diminished circadian gene expression (Zheng et al., 2001). In contrast to wild-type mice, PER1/2 null mice showed no significant difference in their exercise capacity between the Early and Late groups regardless of the exercise protocol (Figures 1E–1G). Consistently, we did not observe any significant difference in their blood glucose levels upon the moderate- and low-intensity exercise protocols between the Early and Late groups (Figures 1F and 1G). Notably, the lack of daily variance in the moderate- and low-intensity exercise protocols in PER1/2 null mice stemmed from reduced performance in the late part (t test, p value 0.00017 and 0.003 for moderate- and low-intensity Late groups, respectively) rather than increased competence at the early part of the active phase in comparison to wild-type mice (t test, $p > 0.05$; compare Figures 1C and 1D with Figures 1F and 1G).

Notably, the food consumption 2 h prior to the exercise test did not significantly differ between the two mouse strains, though we observed an overall tendency for higher food intake in the Early group. The spontaneous locomotor activity of PER1/2 null mice was elevated compared to wild-type mice in the Early group and similar in the Late group (Figure S1A). The total daily food consumption and locomotor activity of wild-type and PER1/2 null mice were comparable (Figure S1B), and the two mouse strains did not differ in their body weight (27.5 ± 1.26; 27.26 ± 0.94, t test, $p = 0.88$, $n = 6$, for wild-type and PER1/2 null mice, respectively).

Taken together, our results suggest that mice exhibit daily variance in exercise capacity that is dependent on exercise intensity and relies on molecular components of the circadian clock.

Time of Day and Exercise Differentially Affect Skeletal Muscle Gene Expression

In view of the intricate nature of exercise biology, it is conceivable that the observed phenotype is the outcome of various effectors both at the system and tissue levels. In the current study, we focused on skeletal muscle (i.e., gastrocnemius), which is known to exhibit significant changes in nutrient demand and energy utilization upon physical activity (Baskin et al., 2015; Egan and Zierath, 2013). The daytime variance in exercise capacity can stem from differences in the starting points, namely the basal metabolic and physiological states that likely differ between the Early and Late groups, and/or be because of differences in the response to exercise between the two time points. In our pursuit for molecular components that are implicated in daily variance of exercise capacity, we considered these two scenarios and analyzed the data accordingly. Hence, to obtain gene expression signatures that capture both the time- and exercise-dependent effects, we characterized the gene expression profiles of mouse gastrocnemius muscle, comparing non-exercised mice (control) with mice performing the moderate-intensity exercise protocol (Exercise) upon which we observed a large difference in exercise capacity between the Early and Late groups. Because there was more than an hour-and-a-half difference in exercise capacity between the two cohorts (Figure 1C), to enable a standardized and well-controlled comparison between the two groups and capture changes that occur throughout the process rather than posteriori, we obtained and analyzed muscle samples from both control and exercised group 1 h from the beginning of the test (Figures 2, 3, S2, and S3; Tables S2 and S3).

As expected, and in line with previous reports of circadian gene expression profiles from skeletal muscle of mice and humans (Andrews et al., 2010; McCarthy et al., 2007; Perrin et al., 2018; Zhang et al., 2014), we observed considerable changes in gene expression in gastrocnemius of sedentary mice between the early and late active phase (time effect), (Figure 2A; Table S2). Overall, 513 transcripts were differentially expressed between the Early and Late groups of non-exercised mice (Figure 2B; Tables S2B and S2C), with 275 and 238 being up- and downregulated, respectively (Figure 2C). Pathway analysis evinced that many of these genes participate in various metabolic pathways and related signaling cascades (e.g., carbohydrate metabolism and peroxisome proliferator-activated receptor [PPAR], AMP-activated protein kinase [AMPK], and hypoxia inducible factor [HIF] signaling pathways), as well as circadian rhythms (Figures

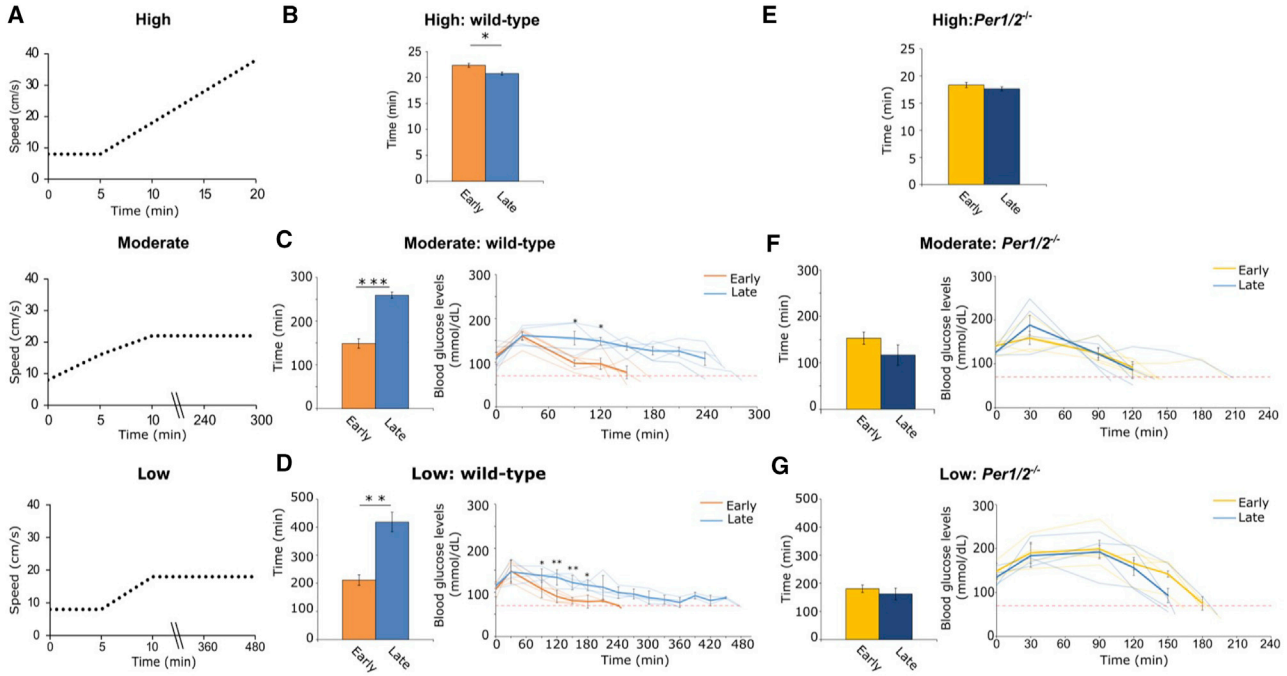

Figure 1. Exercise Capacity Is Daytime Dependent and Clock-Component Regulated

Mice were housed under a 12-h light-dark regimen, and exercise capacity was tested either at the Early or Late part of the dark phase, namely zeitgeber time (ZT) 14 or ZT22, respectively.

(A) Schematic depiction of the different treadmill exercise protocols. High-, moderate-, and low-intensity exercise protocols correspond to 100%, 55%, and 45% of the animals' maximal aerobic capacity, respectively.

(B–D) The running duration of wild-type mice Early and Late upon (B) high-intensity exercise protocol, (C) moderate-intensity exercise protocol (left panel) and their respective blood glucose levels (right panel), and (D) low-intensity exercise protocol (left panel) and their respective blood glucose levels (right panel).

(E–G) The running duration of *Per1/2*$^{-/-}$ mice Early and Late upon (E) high-intensity exercise protocol, (F) moderate-intensity exercise protocol (left panel) and their respective blood glucose levels (right panel), and (G) low-intensity exercise protocol (left panel) and their respective blood glucose levels (right panel). Data are presented as the mean ± SEM of n = 10, 5, and 4 for high, moderate, and low intensity, respectively. *p < 0.05, **p < 0.01, and ***p < 0.001, Student's t test. The exercise tests were performed in constant dark even if mice exceeded the scheduled light-dark regimen.

See also Table S1 and Figure S1.

2D and S2; Table S2E). It is, therefore, conceivable that the basal differences in skeletal muscle gene expression between the Early and Late groups participate in the observed daytime variance in exercise capacity.

Next, we examined the effect of exercise on skeletal muscle gene expression irrespective of the time of the day (exercise effect) (Figure 2; Tables S2C–S2E). Here again, in line with former studies, we observed changes in gene expression upon exercise (Dickinson et al., 2018; Pérez-Schindler et al., 2017). The expression levels of 628 transcripts were altered upon exercise, regardless of the time of day (Figures 2A and 2B), with 313 and 315 being up- and downregulated, respectively (Figure 2C). A subset of transcripts (i.e., 154) was altered by both time and exercise (Figures 2D and 2E; Table S2D). Notably, these common transcripts were enriched for FoxO and insulin signaling (e.g., PI3-AKT), as well as lipid metabolism based on KEGG pathway analysis (Figure 2D), and included several core clock genes (e.g., *Per1*, *Per2*, and *Bmal1*) and master metabolic regulators (e.g., *PPARα* and *KLF10*) (Figure 2E). Intriguingly, the unique transcripts for exercise exhibited remarkable enrichment for immune-related processes such as tumor necrosis factor (TNF) signaling and antigen processing-presenting pathways (Figure 2D; Table S2E).

We concluded that the extent of daytime and exercise effects on gene expression are comparable, whereby some genes are affected by both, for example, several clock genes and master metabolic regulators, whereas others are either exercise or daytime exclusive.

In an attempt to identify genes and pathways that play a role in daily variance in exercise capacity, we dissected the time-dependent effect of exercise on muscle gene expression (Figure 3). Exercise elicited a differential effect on gene expression between the Early and the Late group (503 and 285 for Early and Late group, respectively) (Figures 3A and 3B; Table S2C). In total, 160 genes overlapped between the Early and Late group and hence responded to exercise independently of the time of day (Figure 3B; Table S2F). We observed a daytime-dependent effect on gene expression with an even distribution in the Early group (247 and 256 up- and downregulated, respectively) and a higher propensity of upregulated transcripts in the Late group (178 and 107 up- and downregulated, respectively) (Figure 3C; Table S2C).

KEGG pathway analysis evinced a time-dependent effect between the Early and Late groups upon exercise, whereby insulin signaling pathways and glucose metabolism were enriched

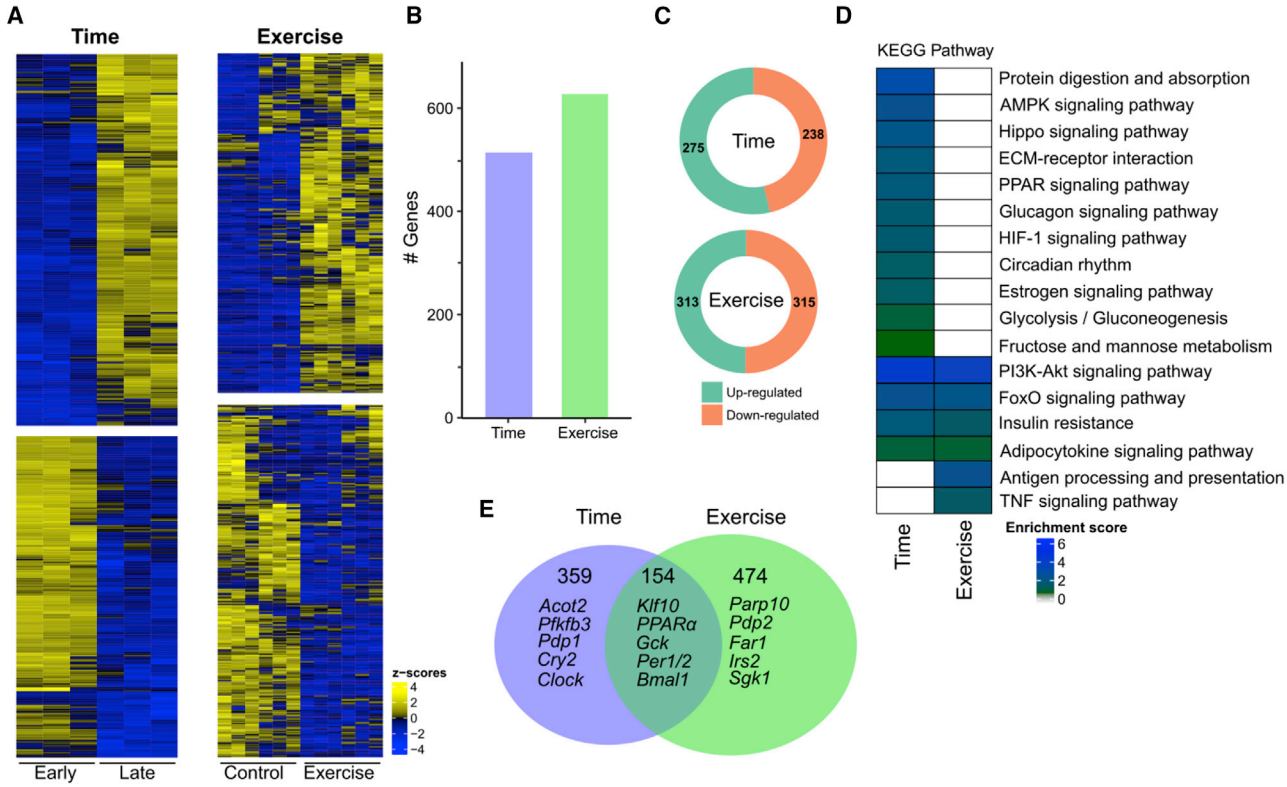

Figure 2. Exercise and Time of Day Differentially Affect Skeletal Muscle Gene Expression

Wild-type mice performed the moderate-intensity exercise protocol either at ZT14 (Early) or ZT22 (Late) for 1 h. Exercised (exercise) and sedentary (control) mice were sacrificed together; the gastrocnemius was dissected; total RNA was prepared and analyzed by RNA-seq.

(A) Heatmap of relative expression of differentially expressed genes between Early and Late sedentary mice (time; left panel) and of differentially expressed genes between sedentary (control, both Early and Late) and exercised (both Early and Late) mice (exercise; right panel). Genes with a positive and negative *Z* scores are depicted in yellow and blue, respectively (EdgeR exact test adjusted FDR < 0.05 and absolute $\log_2$ [fold change] > 0.5, n = 3).

(B) Bar graph representation of the number of genes that were significantly affected by time or exercise.

(C) The number of genes that were significantly up- or downregulated by time or exercise.

(D) KEGG pathway enrichment analysis for time or exercise. The enrichment score ($-\log_{10}$ p value) is depicted in the white-green-blue scale.

(E) Venn diagram depicting the number of unique and overlapping genes between the two groups as well as selected gene names.

See also Tables S2D and S1E and Figure S2.

specifically in the Early group (Figure 3D; Table S2G). Intriguingly, PPARα was induced exclusively in the Early group, which might suggest that this master metabolic regulator is required already at an early stage of the exercise test (i.e., within the first hour) to enable mice to cope with the physical challenge. We also observed an effect on several genes that encode for mitochondrial functions; while the oxidative-phosphorylation-related gene *Coq10b* levels were induced by exercise, regardless of time, both *Atpaf1* and *Atpif1* were repressed upon exercise exclusively in the Early group. By contrast, the mitochondrial uncoupling protein *UCP3* was induced specifically in the Late group (Figure 3E; Table S2C). Thus, exercise alters muscle gene expression in a time-dependent manner, with more pronounced changes in the Early than in the Late group, including a time-specific effect on several metabolic regulators and pathways such as insulin and glucose metabolism.

Since circadian clocks respond to environmental signals, and clocks in peripheral tissues are markedly influenced by metabolic cues (e.g., feeding, temperature, and oxygen) (Asher and Sassone-Corsi, 2015; Reinke and Asher, 2019), we specifically inspected the time- and exercise-dependent effects on the expression levels of core clock genes. In agreement with our RNA sequencing (RNA-seq) data (Table S2), quantitative real-time PCR analyses of core clock transcript levels evinced that some of them respond to exercise in a time-dependent manner (Figure S3; Table S3). As expected, the basal expression levels of the majority of clock genes differed between the two time points, in particular *Per1*, *Per2*, *Clock*, and *Bmal1*, in agreement with their daily rhythmic expression in skeletal muscle (McCarthy et al., 2007; Perrin et al., 2018; Zhang et al., 2014). A trend of induction by exercise was apparent for *Per1*, *Per2, Bmal1*, and *Cry2*. It is noteworthy that *Cry2* expression responds to oxygen levels (Adamovich et al., 2017), which are altered in skeletal muscle upon exercise (Martin et al., 2009). Intriguingly, exercise exclusively induced *Rev-erb*α in the late, but not in the early, part of the active phase.

Collectively, our high-throughput gene expression analyses evinced a distinct muscle gene expression signature that is both daytime and exercise dependent.

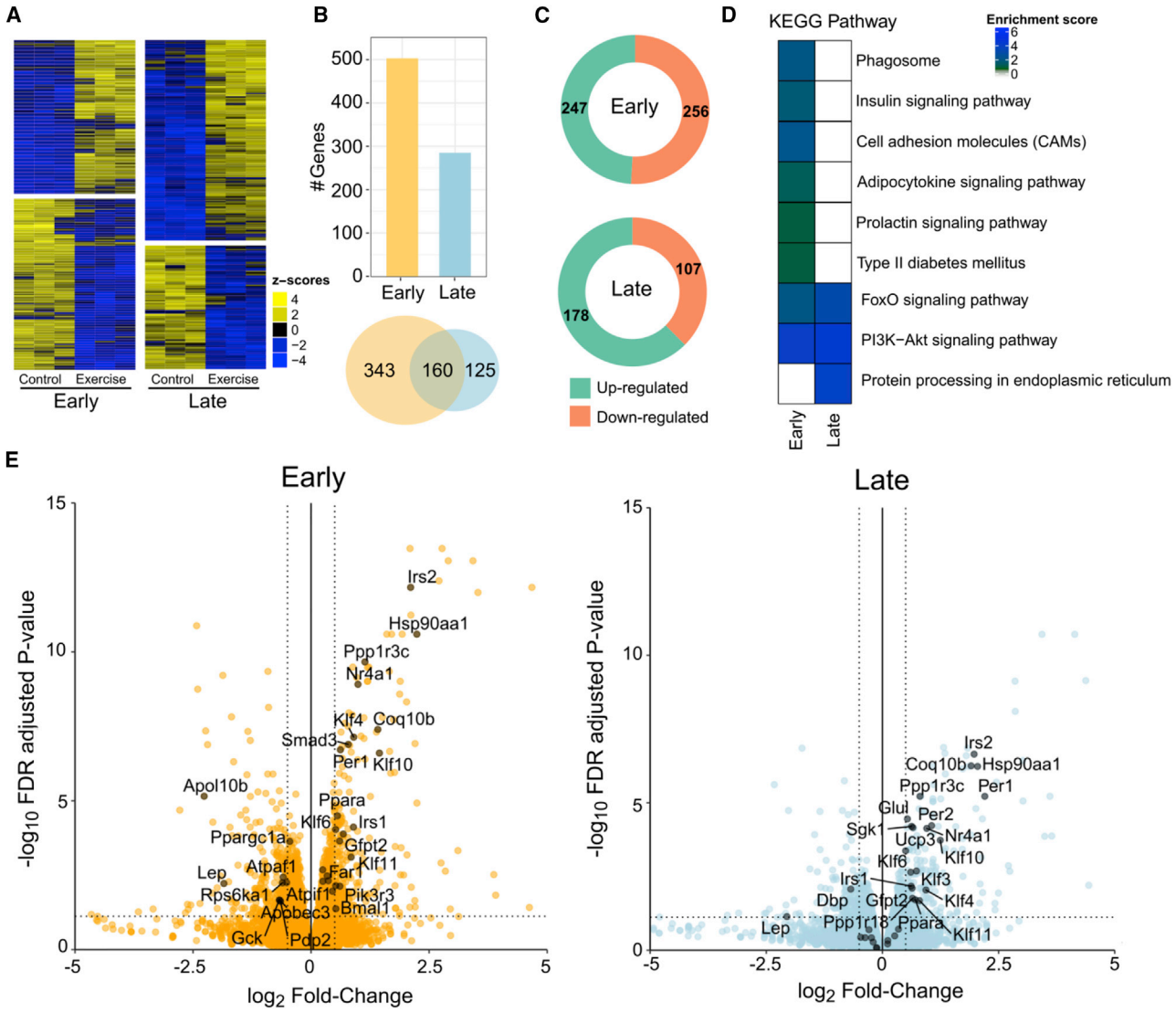

Figure 3. Dissection of the Daytime Effect of Exercise on Skeletal Muscle Gene Expression

(A) Heatmap of relative expression of differentially expressed genes between non-exercised (control) and moderate-intensity exercised mice (exercise) for Early or Late group. Genes with positive and negative *Z* scores are depicted in yellow and blue, respectively (EdgeR exact test adjusted FDR < 0.05 and absolute $\log_2$[fold change] > 0.5, n = 3).

(B) Bar graph representation of the number of genes that were significantly affected by exercise for the Early or Late group with Venn diagram below depicting the number of unique and overlapping genes between the two groups.

(C) The number of genes that were significantly up- or downregulated by exercise in the Early or Late group.

(D) KEGG pathway enrichment analysis for exercise-induced genes for the Early or Late group. The enrichment score ($-\log_{10}$ p value) is depicted in white-green-blue scale.

(E) Volcano plot representation of genes that were significantly affected upon exercise in the Early or Late group. The dotted horizontal and vertical lines represent the significance threshold (Edge R exact test FDR adjusted, $p < 0.05$, and absolute $\log_2$[fold change] > 0.5, respectively; n = 3). Names of selected genes are indicated.

See also Table S2 and Figure S3.

Dissection of Daytime and Exercise Effect on Skeletal Muscle Metabolic Profile

At the molecular level, it is well known that exercise induces substantial changes on skeletal muscles at multiple levels from a transcriptional response to marked changes in metabolite content, metabolic pathway activation, and energy utilization (Egan and Zierath, 2013; Overmyer et al., 2015; Starnes et al., 2017). Likewise, circadian changes in metabolite composition of muscle tissue were recently reported (Dyar et al., 2018a, 2018b). The above-described high-throughput gene expression analyses depicted the daytime- and exercise-dependent effects on the transcriptional response. To obtain a comprehensive view of the molecular events that occur in skeletal muscle upon physical activity and conceivably account for the daytime

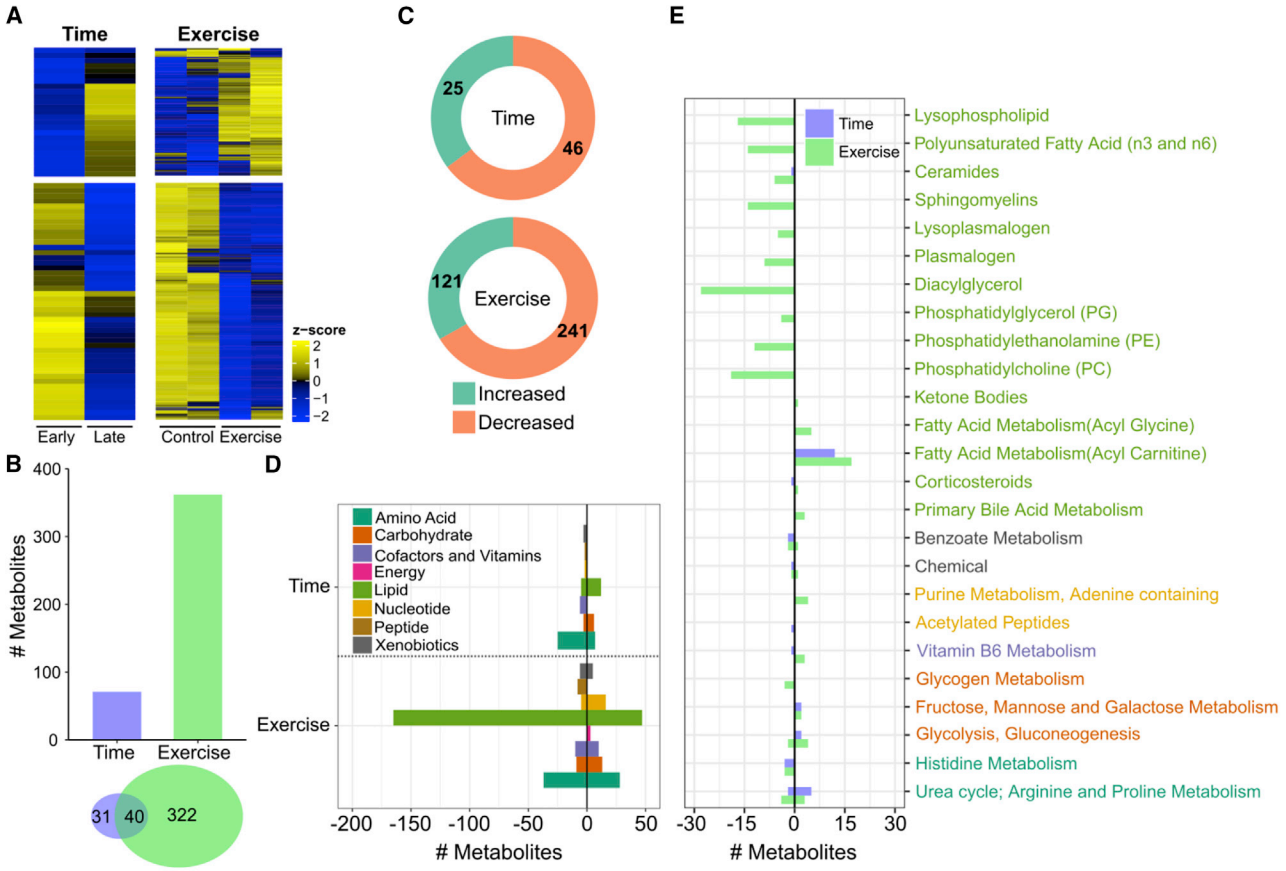

Figure 4. Exercise and Daytime Differentially Affect Skeletal Muscle Metabolic Profile

Wild-type mice performed the moderate-intensity exercise protocol either at ZT14 (Early) or ZT22 (Late) for 1 h. Exercised (exercise) and sedentary (control) mice were sacrificed together, the gastrocnemius was dissected, and metabolomics analysis was performed.

(A) Heatmap of relative metabolite levels between Early and Late sedentary mice (time; left panel) and between sedentary (control, both Early and Late) and exercised (both Early and Late) mice (exercise; right panel). Significant metabolites with positive and negative *Z* scores are depicted in yellow and blue, respectively (ANOVA, $p < 0.05$, mean of $n = 8$).

(B) Bar graph representation of the number of metabolites that were significantly affected by time or exercise with Venn diagram below depicting the number of unique and overlapping metabolites between the two groups.

(C) Overall number of metabolites that were significantly increased or decreased by time or exercise.

(D) The number of metabolites that were significantly increased or decreased by time or exercise is plotted according to the different types (see color code).

(E) The number of metabolites that were significantly increased or decreased by time or exercise grouped according to metabolic pathways that were identified in our enrichment analysis (Table S4D). Names are marked according to the type color code as in (D).

See also Figure S4 and Table S4.

variance in exercise capacity, we complemented the transcriptomic analyses with metabolic profiling of skeletal muscle under the same experimental conditions as aforementioned for the transcriptomic analyses (Figures 4, 5, S4, and S5; Table S4).

Overall, 613 named metabolites were detected in the gastrocnemius tissue samples. In total, 71 metabolites differed between the Early and Late group of non-exercised animals (time effect), with 46 decreased and 25 increased (Figures 4A–4C and S4A). These mostly include amino acids and lipids (Figure 4D). Next, we examined the effect of exercise on muscle metabolic profile irrespective of daytime (exercise effect). The levels of 362 metabolites were altered, regardless of daytime (Figures 4A and 4B; Table S4B), with 121 and 241 being up- and downregulated, respectively (Figure 4C). Exercise induced prominent changes in the muscle lipid content and, to a lesser extent, affected amino acid, carbohydrate, and nucleotide levels (Figure 4D). We identified 40 metabolites that were affected by both the time of day and exercise and mostly included acyl-carnitines (e.g., hexanoylcarnitine, hydroxyhexanoylcarnitine, octanoylcarnitine, 5-dodecenoylcarnitine, laurylcarnitine, myristoylcarnitine, and palmitoylcarnitine) as well as several amino acids (e.g., phenylalanine, leucine, methionine, cysteine, and arginine) (Figure 4B; Table S4C). A detailed analysis of different enriched subtypes of metabolites that were altered either upon time of day or exercise showed a prominent increase in consumption of different lipids alongside an increase in acyl-carnitines upon exercise, which is consistent with elevated fatty acid oxidation upon physical activity (Figure 4E; Table S4D).

Overall, our analysis evinced that exercise elicits more pronounced changes on the muscle metabolic profile compared

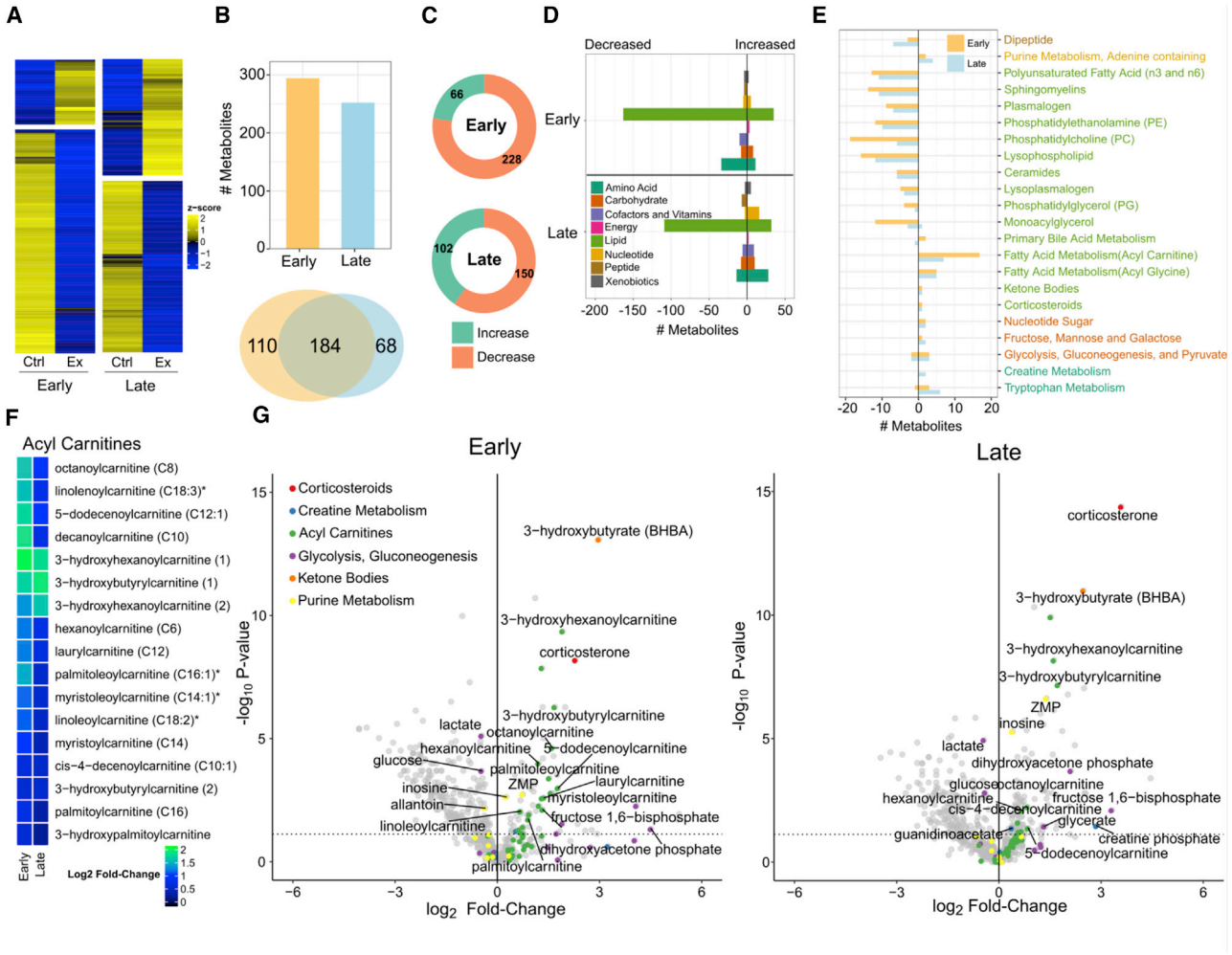

Figure 5. Dissection of the Daytime Effect of Exercise on Skeletal Muscle Metabolic Profile

(A) Heatmap of relative metabolite levels between non-exercised (Ctrl) and moderate-intensity exercised mice (Ex) for Early or Late group. Significant metabolites with positive and negative *Z* scores are depicted in yellow and blue, respectively (ANOVA, $p < 0.05$, mean of n = 8).

(B) Bar graph representation of the number of metabolites that were significantly affected by exercise for the Early or Late group with Venn diagram below depicting the number of unique and overlapping metabolites between the two groups.

(C) The number of metabolites that were significantly increased or decreased by exercise in the Early or Late group.

(D) The number of metabolites that were significantly increased or decreased by exercise in the Early or Late group is plotted according to the different types (see color code).

(E) The number of metabolites that were significantly increased or decreased by exercise in the Early or Late groups, arranged according to metabolic pathways that were identified in our enrichment analysis (Table S4F). Names are marked according to the type color code as in (D).

(F) Heatmap of relative acyl-carnitine levels (log_2[fold change] exercise/control) significantly affected by exercise in the Early or Late group (ANOVA, $p < 0.05$, mean of n = 8).

(G) Volcano plot representation of metabolites that were significantly affected upon exercise in the Early or Late group. The dotted horizontal line represents the significance threshold (ANOVA, $p < 0.05$, n = 8). Names of selected metabolites are indicated.

See also Table S4E and Figure S5.

to daytime, in particular, with respect to muscle lipid composition. This is in contrast to the above-described effects of time or exercise on gene expression, whereby we observed comparable changes (compare Figure 2 with Figure 4).

To identify metabolic pathways and metabolites that potentially play a role in the observed daytime variance in exercise capacity, we analyzed the time-dependent effect of exercise on muscle metabolite composition (Figure 5). Exercise induced changes in metabolite levels with 294 and 252 metabolites for the Early and Late groups, respectively, with a higher propensity of metabolites that were decreased in both groups (Figures 5A–5C; Table S4B). Comparison between the Early and Late groups evinced that, upon exercise, the Early group exhibited a more pronounced decrease in lipids and amino acids than in the Late group (Figure 5D; Table S4E). More specifically, the prominent lipid consumption was accompanied by an increase in acylcarnitines in the Early compared to the Late group (Figures 5E–5G; Tables S4E and S4F). Notably, 17 out of 38 (~45%)

acyl-carnitines detected in our metabolomics were significantly affected by exercise in the Early group (palmitoylcarnitine [C16] and its breakdown derivatives decanoylcarnitine [C10], octanoylcarnitine [C8], and hexanoylcarnitine [C6]), suggesting incomplete fatty acid oxidation and mitochondrial overload (Koves et al., 2008) that is consistent with a lower exercise capacity (Overmyer et al., 2015).

A detailed analysis of the individual metabolites enabled us to identify significantly altered metabolites that are known to play a role in metabolic control. 5-aminoimidazole-4-carboxamide ribonucleotide (ZMP) and corticosterone were of particular interest, as detailed below (Figure 5G). Interestingly, corticosterone was significantly elevated upon exercise with a prominent time-dependent effect (Figure S5). This increase in corticosterone could account for the observed increase in free fatty acid consumption and consequently β-oxidation. The differential time response upon exercise suggests that this is not merely due to a stress response to the protocol applied. The levels of corticosterone in control non-exercised mice were higher for the Early than in the Late group, in agreement with the reported daily rhythmicity in corticosterone levels (Atkinson and Waddell, 1997).

Collectively, our analyses evinced a specific metabolic signature for skeletal muscle that is daytime and exercise dependent.

Time- and Exercise-Dependent ZMP Accumulation, AMPK Activation, and Metabolic Consequences

Our metabolomics analyses revealed that ZMP levels are elevated upon exercise, with peak levels observed for the Late group (Figure 6A). ZMP is produced upon *de novo* purine and histidine biosynthesis and is known to act as an allosteric activator of the master cellular energy sensor AMPK, (Burkewitz et al., 2014). It can act either endogenously (Asby et al., 2015) or exogenously when administered as the corresponding cell-permeable ribonucleoside (AICAR) (Corton et al., 1995). The latter has been shown to improve exercise performance both in mice and humans (Fan and Evans, 2017; Narkar et al., 2008). Upon AMPK activation, it promotes fatty acid oxidation and muscle remodeling. AMPK signaling extends through a myriad of pathways to replenish cellular ATP levels through repression of anabolic pathways and activation of catabolic pathways (Mihaylova and Shaw, 2011).

To probe the effect of the rise in endogenous ZMP levels in skeletal muscle, we tested by immunoblot, the major regulatory event of AMPK activation, namely its phosphorylation at Thr172 (Hawley et al., 1996). Consistent with ZMP levels, we observed an increase in AMPK Thr172 phosphorylation upon exercise, with peak levels in the Late group (Figure 6B). Liver kinase B1 (LKB1) is a major kinase phosphorylating AMPK under conditions of energy stress (Shackelford and Shaw, 2009). PKCζ phosphorylates Ser428 of LKB1 and exports it to the cytosol, which is essential for AMPK activation. We did not observe significant changes in LKB1 phosphorylation, supporting the possibility of AMPK activation through allosteric activation by ZMP (Figure 6B).

Finally, previous gene expression profiling identified a subset of genes that are activated by the exogenously administered derivate of ZMP, i.e., the cell-permeable ribonucleoside AICAR (Narkar et al., 2008). Therefore, to examine the extent of the downstream effects of AMPK activation by exercise-induced ZMP levels, we analyzed their transcript levels by quantitative real-time PCR (Figure S6; Tables S5A and S5B). In agreement with our RNA-seq data (Table S2B), we did find that several of these transcripts (e.g., *Fasn*, *Scd1*, and *Fabp3*) generally respond in accordance with the observed increase in ZMP levels and AMPK activation.

Taken together, our findings support ZMP activation of AMPK upon exercise in a daytime-dependent manner with peak activation in the late part of the active phase. The metabolic consequences of AMPK activation are stimulation of glycolysis and inhibition of lipid synthesis as well as activation of fatty acid β-oxidation (Jeon, 2016; Shackelford and Shaw, 2009). Thus, as expected from the increase in energy demand upon exercise, changes in glycolytic intermediates were evident both for the Early and Late groups. Specifically, the decrease in glucose levels upon exercise was accompanied by elevated glycolytic intermediates such as glucose 6-phosphate, fructose 1,6-biphosphate, phosphoenolpyruvate, and dihydroxyacetone-phosphate more in the Late group (Figure 6C; Table S4B). In addition, we observed a signature of elevated β-oxidation in the muscle tissue upon exercise (Figure 6D). The rate of β-oxidation is controlled by mitochondrial uptake of fatty acids using the carnitine shuttle, which removes fatty acyl-CoA from the cytosol and generates fatty acyl CoA in the mitochondrial matrix that can then be utilized for β-oxidation and ATP generation. In this conjuncture, we previously showed that mitochondrial nutrient utilization is circadian clock controlled (Neufeld-Cohen et al., 2016). As noted above, the consumption of different fatty acids (e.g., palmitate [16:0]) and carnitine upon exercise was associated with increased levels of acyl-carnitines (e.g., palmitoylcarnitine [C16], decanoylcarnitine [C10], butyrylcarnitine [C4], and propionylcarnitine [C3]) more in the Early than in the Late group, hinting toward less efficient fatty acid oxidation in the Early group (Figure 6D; Table S4B).

Overall, we observed changes in substrate utilization upon exercise in respect to glycolysis and fatty acid oxidation that are exercise dependent and to some extent daytime regulated. These changes might be driven in part through ZMP-AMPK activation and potentially play a role in the daily variance of exercise capacity.

Daily Variance in Physiological Parameters upon Exercise in Humans

Our finding that mice exhibit daily variance in exercise capacity encouraged us to test whether this holds as well in humans. Young, healthy individuals (anthropometric data are listed in Table S7) were subjected to submaximal constant-load exercise protocol (Figure 7A), the equivalent of the moderate-intensity exercise protocol in mice. Each participant performed the exercise protocol on two occasions, at 8.00 a.m. (Early) and 6.00 p.m. (Late), separated by a minimum interval of 2.5 days. Subjects refrained from physical activity the day before and the day of the test, slept for at least 7 h the night before the tests, abstained from drinking caffeinated beverages and alcohol on test days, and had a standardized meal 2 h prior to the tests. Oxygen consumption and carbon dioxide release, as well as heart rate, ventilation, body temperature, and blood glucose and lactate levels, were monitored before (time 0) and throughout the exercise protocol (Figure 7).

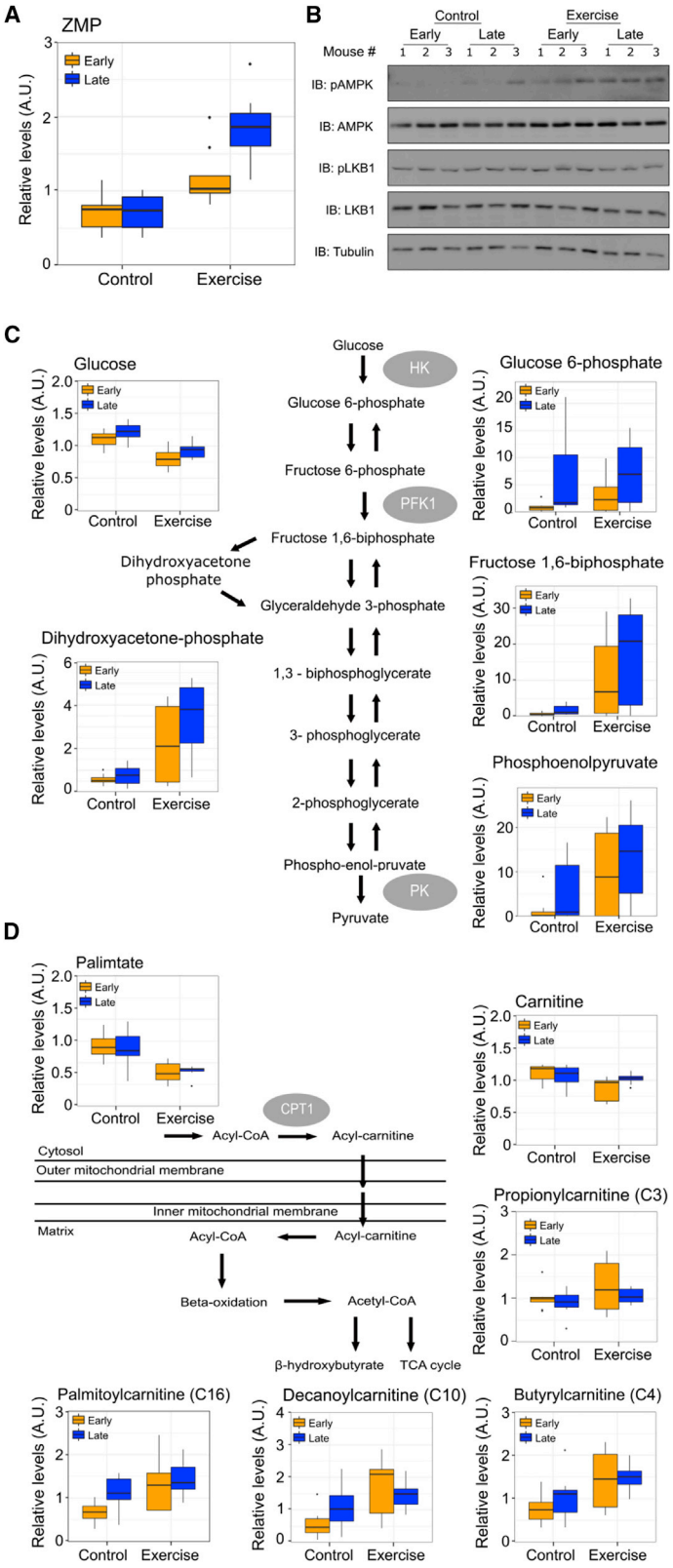

Figure 6. Time- and Exercise-Dependent ZMP Accumulation, AMPK Activation, and Metabolic Consequences

Wild-type mice performed the moderate-intensity exercise protocol either at ZT14 (Early) or ZT22 (Late) for 1 h. Exercised (exercise) and non-exercised (control) mice were sacrificed together; the gastrocnemius was dissected and analyzed.

(A) ZMP levels in gastrocnemius tissue samples for Early and Late group of non-exercised and exercised animals.

(B) Protein extracts were prepared from gastrocnemius tissue and analyzed by SDS-PAGE and immunoblot (IB) with indicated antibodies.

(C) Schematic representation of key enzymatic steps in glycolysis with quantification of relevant metabolites.

(D) Schematic representation of key enzymatic steps in fatty acid mitochondrial import and oxidation with quantification of relevant metabolites. Metabolite levels are presented in boxplots; center indicates the median, and the bottom and top edges indicate the 25th and 75th percentiles, with 8 animals per group.

a.u., arbitrary units; ZMP, 5-aminoimidazole-4-carboxamide ribonucleotide; HK, hexokinase; PFK1, phosphofructokinase 1; PK, pyruvate kinase; CPT-1, carnitine palmitoyltransferase I.

See also Table S5 and Figure S6.

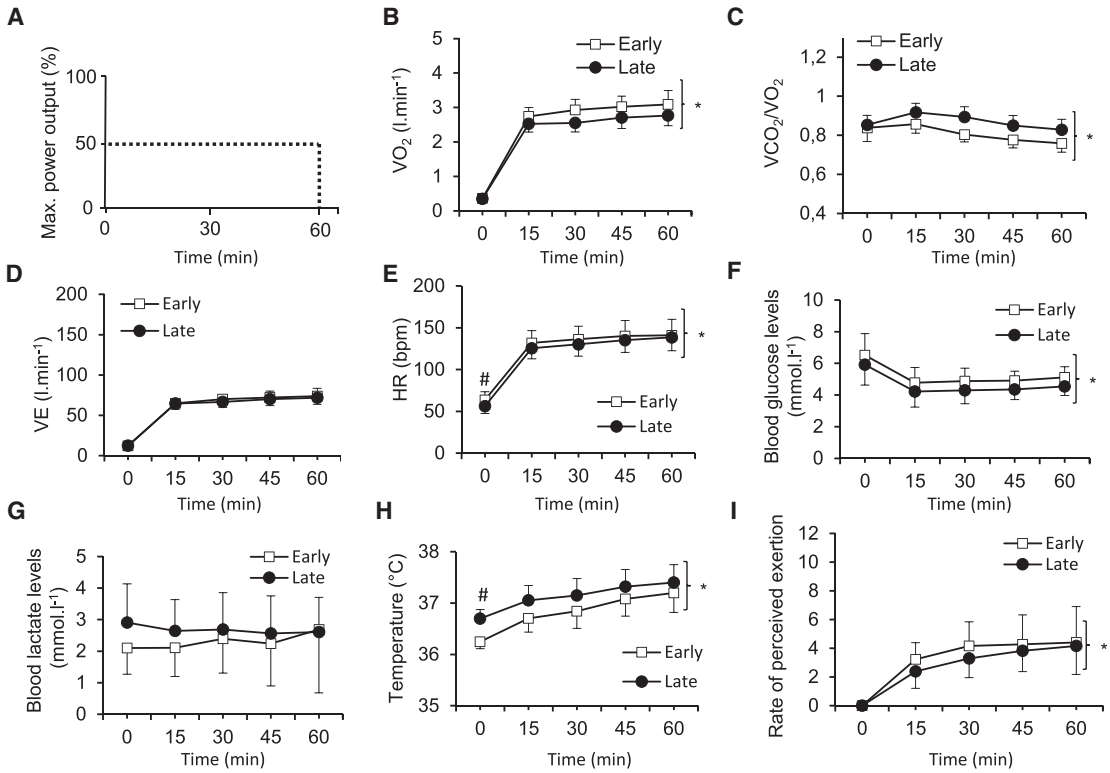

Figure 7. Daily Variance in Physiological Parameters upon Exercise in Humans

Physiological parameters were monitored before (time 0) and during submaximal constant load (i.e., 50% of the individual maximal power output as detailed in Table S7) exercise test for 1 h in humans at 8:00 a.m. and at 6:00 p.m. (i.e., Early and Late, respectively).

(A) Schematic depiction of the submaximal constant-load exercise test.

(B) Oxygen consumption.

(C) Respiratory exchange ratio (RER) (VCO_2/VO_2).

(D) Minute ventilation (VE).

(E) Heart rate (HR).

(F) Blood glucose levels.

(G) Blood lactate levels.

(H) Body temperature as measured intra-auricular.

(I) The rate of perceived exertion. Data are presented as mean ± SD of n = 12. The time-of-day effect on rest measurements (time 0) was analyzed by t test; #$p < 0.05$. The effect of exercise and time of day (Early versus Late) was analyzed by a two-way repeated measures ANOVA, *$p < 0.05$. Anthropometric information and the experimental design are detailed in the STAR Methods.

See also Table S7.

We found that oxygen consumption was significantly lower in the Late than in the Early upon the exercise protocol (Figure 7B), whereas the respiratory exchange ratio (RER) (i.e., carbon dioxide production/oxygen consumption) was significantly higher in the Late than in Early (Figure 7C). By contrast, no significant difference in oxygen consumption and RER between the Early and Late was observed at rest (time 0) suggesting that these effects are exercise dependent.

We did not observe significant changes in ventilation between the Early and Late (Figure 7D). Heart rate was lower in the Late before and throughout the exercise protocol (Figure 7E). Blood glucose levels were higher in Early than in Late upon exercise (Figure 7F), and there were no significant differences in blood lactate levels between the Early and Late (Figure 7G). Consistent with the daily changes in body temperature, which reaches its zenith level late in the active phase (Weinert and Waterhouse, 2007), we found that body temperature was significantly higher in Late than in Early (Figure 7H). Finally, the rate of perceived exertion differed between the two time points and was lower in the Late (Figure 7I).

We concluded that the lower oxygen consumption upon exercise in Late compared to Early support a better exercise efficiency in humans (i.e., a lower oxygen consumption for a given mechanical power output) in the late compared to the early part of the active phase. These results are in line with the above-described exercise tests (i.e., moderate-intensity protocol) performed with mice.

DISCUSSION

In this study, we examined the temporal variance in exercise capacity at the physiological and molecular levels. In essence, we found that both mice and humans exhibit daytime variance in exercise capacity between the early and late part of their active

phase. The daytime variance in mice was exercise-intensity dependent and relied on the clock proteins PER1/2. At the molecular level, we applied high-throughput transcriptomic and metabolomics on skeletal muscle and identified a variety of daytime- and exercise-dependent effects, several of which may account for the observed differences in exercise capacity. In view of the intricate nature of exercise biology, it is conceivable that exercise capacity is determined by a multitude of parameters at multiple levels (Egan and Zierath, 2013; Hawley et al., 2014). Here, we focused on skeletal muscle, a major determinant of exercise capacity, and obtained a distinct daytime and exercise transcriptomic and metabolic signatures. Overall, at the transcriptome level, the exercise effect was comparable to the daytime effect, whereas at the metabolic level, the exercise effect was much more prominent. It is likely that the metabolic changes occur more rapidly prior to the transcriptional changes and therefore were more apparent within the first hour of our measurements.

Circadian Clocks and Exercise Capacity

Circadian clocks regulate almost every aspect of our physiology and behavior among other rest-activity and feeding-fasting cycles. Consequently, food intake and spontaneous activity prior to the exercise protocols do differ between the cohorts tested in the early compared to the late part of the day, as the former had just begun their active phase and the latter had been already active and had ingested food several hours previously. Likewise, hormone levels, as well as a wide variety of physiological parameters, vary. As the premise of our work is that the conjunction of these parameters affect exercise capacity and because feeding and activity strongly affect the circadian clock (Bass and Lazar, 2016; Bass and Takahashi, 2010; Panda, 2016), we refrained from interfering with the animals' activity or feeding behavior prior to the exercise test and thus preserved their natural rhythms.

The daily variance in exercise capacity was dependent on PER1/2, which are components of the repressor arm of the circadian clock (Nangle et al., 2014). It raises the possibility that the circadian clock is implicated in exercise biology. Future studies, with additional clock-deficient mouse models, are expected to clarify the role of the circadian clock versus clock proteins in the control of exercise capacity. In this conjuncture, recently it was shown that the circadian repressors CRY1 and CRY2 function as co-repressors for PPARδ and modulate exercise capacity (Jordan et al., 2017). In turn, we do observe an effect of exercise on the expression levels of several clock genes. This raises the intriguing possibility that exercise can serve as an external timing cue (ZT) for circadian clocks and might shape circadian gene expression. Along this line, Sassone-Corsi and coworkers applied high-throughput transcriptomics and metabolomics to characterize the effect of exercise, either in the rest or the active phase, on circadian gene expression and metabolic profiles (see accompanying paper by Sato et al., 2019 in this issue of *Cell Metabolism*). Thus, it appears that there is crosstalk between exercise and the circadian clock.

Time- and Exercise-Dependent ZMP Accumulation and AMPK Activation

The distinct daytime and exercise-type transcriptomic and metabolic signature in skeletal muscle point toward a difference in nutrient utilization and metabolic pathway activation, in particular, fatty acid oxidation and glycolysis. As mentioned above, AMPK is a master metabolic sensor that activates a myriad of pathways to replenish cellular ATP levels through repression of anabolic pathways and induction of catabolic pathways. Remarkably, we discovered that ZMP, an endogenous AMPK activator, is induced by exercise in a time-dependent manner. It is, therefore, plausible that the observed daytime and exercise differences in nutrient utilization are, in part, regulated by ZMP through AMPK activation. In line with this notion, we did not observe significant differences in LKB phosphorylation. Yet we cannot exclude that alternate signaling pathways besides ZMP or even regardless of AMPK, for example, through corticosterone levels, also play a role in the observed metabolic shift in nutrient utilization. It is notable that AMPK was reported to phosphorylate and destabilize CRY1 (Lamia et al., 2009), which in turn by itself can modulate exercise capacity through PPARδ (Jordan et al., 2017), adding another layer of intersection between the metabolic sensing mechanism, clock components, and exercise capacity.

Daytime Variance in Exercise Capacity in Humans

Our human study supports the idea that time of the day affects exercise capacity likely through differences in exercise metabolic response. The lower oxygen consumption upon exercise Late compared to Early suggests a better exercise efficiency in humans in the evening hours. This is in line with previous studies showing better exercise capacity in the evening than in the morning hours in humans (Drust et al., 2005; Küüsmaa et al., 2016; Reilly and Waterhouse, 2009; Thosar et al., 2018).

The improved exercise efficiency Late compared to Early was associated with a greater reliance on carbohydrates (as indicated by the higher RER). Carbohydrates require less oxygen per amount of ATP produced, which may contribute to the lower oxygen consumption and lower glycemia upon exercise, Late compared to Early. Lower oxygen consumption is also expected to be associated with reduced cardiovascular responses (as illustrated by the lower heart rate) and rate of perceived exertion as observed Late compared to Early. Higher body temperature during exercise Late compared to Early was previously reported and may contribute to improved neuromuscular function and subsequently exercise capacity (Ammar et al., 2017). Overall, these results support a daytime effect as well on metabolic responses to exercise as observed in mice.

Future Directions and Perspectives

The approach applied herein, namely testing the daytime effect on exercise capacity in conjunction with comprehensive comparative analyses (i.e., transcriptomics and metabolomics), emerges as a valuable tool for identifying potential factors that are implicated in determining exercise capacity. Thus, it provides a proof of principle that can be expanded to a wide variety of functions that differ throughout the day.

Our work sets the stage for subsequent studies addressing the daytime effect on exercise. We specifically examined the daily variance in exercise capacity, yet as aforementioned, exercise is a major benefactor for human health. In this conjuncture, it would be interesting to determine whether the time of the day also affects the metabolic benefits associated with exercise

such as weight loss and insulin resistance. In parallel to the growing interest in chronotherapy and chrononutrition, characterizing the chrono-exercise effect, namely depicting the best time of the day for different types of physical activities and their respective outcomes (capacity- and health-wise) is highly appealing.

Limitations of Study

The current study relies on muscle transcriptomics and metabolomics to identify molecular events that play a role in daily variance in exercise capacity. Metabolic flux analysis in conjunction with kinetic experiments, though technically challenging and laborious, are expected to provide a more accurate and detailed depiction of the metabolic events that occur upon exercise in a daytime-dependent manner. In addition, we do not exclude the likelihood that the observed phenotype stems from various effectors including the cardiovascular system as well as liver and adipose tissue function, which are known to exhibit daily rhythmicity and affect exercise performance. Lastly, our finding that the PER1/2 null mice, unlike wild-type mice, do not exhibit daily variance in exercise capacity raises an open question of whether the observed phenotype is circadian clock dependent or rather related to PER proteins' function as transcriptional repressors.

STAR★METHODS

Detailed methods are provided in the online version of this paper and include the following:

- KEY RESOURCES TABLE
- CONTACT FOR REAGENT AND RESOURCE SHARING
- EXPERIMENTAL MODEL AND SUBJECT DETAILS
  - Animals
  - Human Subjects - Exclusion and Inclusion Criteria
- METHOD DETAILS
  - Mouse Exercise Protocols
  - Animals Activity and Food Consumption Measurements
  - Sample Preparation for RNA-seq, Metabolomics, and Protein Analyses
  - RNA Preparation for RNA-seq and Real-Time PCR Analysis
  - RNA-seq Data Processing and Analysis
  - Real-Time PCR Analysis
  - Protein Extraction, Gel Electrophoresis and Immunoblotting
  - Metabolomics Sample Preparation, Quality Control, Data Extraction and Analysis
  - Metabolite Set Enrichment Analysis
  - Human Exercise Protocols
  - Measurements and Statistical Analysis of Human Exercise Performance
- QUANTIFICATION AND STATISTICAL ANALYSIS
- DATA AND SOFTWARE AVAILABILITY

SUPPLEMENTAL INFORMATION

Supplemental Information can be found online at https://doi.org/10.1016/j.cmet.2019.03.012.

ACKNOWLEDGMENTS

We are grateful to the members of the Asher lab for their valuable comments on the manuscript. We thank Beni Sioani for his assistance with the animal care and Asher Auerbach for his technical support. G.A. is supported by the European Research Council (ERC-2017 CIRCOMMUNICATION 770869) and is a recipient of the EMBO young investigator award. The work done in the S.V. lab is supported by the "Fonds de dotation AGIR pour les maladies chroniques" and by the French National Research Agency (ANR-12-TECS-0010) in the framework of the "Investissements d'avenir" program (ANR-15-IDEX-02). J.S. is a recipient of a fellowship from the Placide Nicod Foundation.

AUTHOR CONTRIBUTIONS

Conceptualization, S.E., Z.Z., and G.A.; Investigation, S.E., Z.Z., S.B., S.D., B.L., and M.G.; Visualization, S.E., J.S., and S.V.; Data Curation, J.S.; Software, J.S.; Funding, G.A.; Writing – Review & Editing, S.E., J.S., S.V., and G.A.

DECLARATION OF INTERESTS

The authors declare no competing interests.

Received: August 30, 2018
Revised: February 6, 2019
Accepted: March 20, 2019
Published: April 18, 2019

REFERENCES

Adamovich, Y., Ladeuix, B., Golik, M., Koeners, M.P., and Asher, G. (2017). Rhythmic oxygen levels reset circadian clocks through HIF1alpha. Cell Metab. *25*, 93–101.

Adamovich, Y., Ladeuix, B., Sobel, J., Manella, G., Neufeld-Cohen, A., Assadi, M.H., Golik, M., Kuperman, Y., Tarasiuk, A., Koeners, M.P., et al. (2019). Oxygen and carbon dioxide rhythms are circadian clock controlled and differentially directed by behavioral signals. Cell Metab. https://doi.org/10.1016/j.cmet.2019.01.007.

Ammar, A., Chtourou, H., and Souissi, N. (2017). Effect of time-of-day on biochemical markers in response to physical exercise. J. Strength Cond. Res. *31*, 272–282.

Anders, S., Pyl, P.T., and Huber, W. (2015). HTSeq–a Python framework to work with high-throughput sequencing data. Bioinformatics *31*, 166–169.

Andrews, J.L., Zhang, X., McCarthy, J.J., McDearmon, E.L., Hornberger, T.A., Russell, B., Campbell, K.S., Arbogast, S., Reid, M.B., Walker, J.R., et al. (2010). CLOCK and BMAL1 regulate MyoD and are necessary for maintenance of skeletal muscle phenotype and function. Proc. Natl. Acad. Sci. USA *107*, 19090–19095.

Asby, D.J., Cuda, F., Beyaert, M., Houghton, F.D., Cagampang, F.R., and Tavassoli, A. (2015). AMPK activation via modulation of de novo purine biosynthesis with an inhibitor of ATIC homodimerization. Chem. Biol. *22*, 838–848.

Asher, G., and Sassone-Corsi, P. (2015). Time for food: the intimate interplay between nutrition, metabolism, and the circadian clock. Cell *161*, 84–92.

Atkinson, H.C., and Waddell, B.J. (1997). Circadian variation in basal plasma corticosterone and adrenocorticotropin in the rat: sexual dimorphism and changes across the estrous cycle. Endocrinology *138*, 3842–3848.

Baskin, K.K., Winders, B.R., and Olson, E.N. (2015). Muscle as a "mediator" of systemic metabolism. Cell Metab. *21*, 237–248.

Bass, J., and Lazar, M.A. (2016). Circadian time signatures of fitness and disease. Science *354*, 994–999.

Bass, J., and Takahashi, J.S. (2010). Circadian integration of metabolism and energetics. Science *330*, 1349–1354.

Burkewitz, K., Zhang, Y., and Mair, W.B. (2014). AMPK at the nexus of energetics and aging. Cell Metab. *20*, 10–25.

Cartee, G.D., Hepple, R.T., Bamman, M.M., and Zierath, J.R. (2016). Exercise promotes healthy aging of skeletal muscle. Cell Metab. *23*, 1034–1047.

Corton, J.M., Gillespie, J.G., Hawley, S.A., and Hardie, D.G. (1995). 5-amino-imidazole-4-carboxamide ribonucleoside. A specific method for activating AMP-activated protein kinase in intact cells? Eur. J. Biochem. *229*, 558–565.

Dibner, C., Schibler, U., and Albrecht, U. (2010). The mammalian circadian timing system: organization and coordination of central and peripheral clocks. Annu. Rev. Physiol. *72*, 517–549.

Dickinson, J.M., D'Lugos, A.C., Naymik, M.A., Siniard, A.L., Wolfe, A.J., Curtis, D.R., Huentelman, M.J., and Carroll, C.C. (2018). Transcriptome response of human skeletal muscle to divergent exercise stimuli. J. Appl. Physiol. *124*, 1529–1540.

Distefano, G., and Goodpaster, B.H. (2018). Effects of exercise and aging on skeletal muscle. Cold Spring Harb. Perspect. Med. *8*, https://doi.org/10.1101/cshperspect.a029785.

Dobin, A., Davis, C.A., Schlesinger, F., Drenkow, J., Zaleski, C., Jha, S., Batut, P., Chaisson, M., and Gingeras, T.R. (2013). STAR: ultrafast universal RNA-seq aligner. Bioinformatics *29*, 15–21.

Drust, B., Waterhouse, J., Atkinson, G., Edwards, B., and Reilly, T. (2005). Circadian rhythms in sports performance–an update. Chronobiol. Int. *22*, 21–44.

Dyar, K.A., Hubert, M.J., Mir, A.A., Ciciliot, S., Lutter, D., Greulich, F., Quagliarini, F., Kleinert, M., Fischer, K., Eichmann, T.O., et al. (2018a). Transcriptional programming of lipid and amino acid metabolism by the skeletal muscle circadian clock. PLoS Biol. *16*, e2005886.

Dyar, K.A., Lutter, D., Artati, A., Ceglia, N.J., Liu, Y., Armenta, D., Jastroch, M., Schneider, S., de Mateo, S., Cervantes, M., et al. (2018b). Atlas of circadian metabolism reveals system-wide coordination and communication between clocks. Cell *174*, 1571–1585.e11.

Egan, B., and Zierath, J.R. (2013). Exercise metabolism and the molecular regulation of skeletal muscle adaptation. Cell Metab. *17*, 162–184.

Evans, A.M., DeHaven, C.D., Barrett, T., Mitchell, M., and Milgram, E. (2009). Integrated, nontargeted ultrahigh performance liquid chromatography/electrospray ionization tandem mass spectrometry platform for the identification and relative quantification of the small-molecule complement of biological systems. Anal. Chem. *81*, 6656–6667.

Fan, W., and Evans, R.M. (2017). Exercise mimetics: impact on health and performance. Cell Metab. *25*, 242–247.

Fan, W., Waizenegger, W., Lin, C.S., Sorrentino, V., He, M.X., Wall, C.E., Li, H., Liddle, C., Yu, R.T., Atkins, A.R., et al. (2017). PPARδ promotes running endurance by preserving glucose. Cell Metab *25*, 1186–1193.e4.

Fresno, C., and Fernández, E.A. (2013). RDAVIDWebService: a versatile R interface to David. Bioinformatics *29*, 2810–2811.

Gabriel, B.M., and Zierath, J.R. (2017). The limits of exercise physiology: from performance to health. Cell Metab. *25*, 1000–1011.

Hawley, J.A., Hargreaves, M., Joyner, M.J., and Zierath, J.R. (2014). Integrative biology of exercise. Cell *159*, 738–749.

Hawley, S.A., Davison, M., Woods, A., Davies, S.P., Beri, R.K., Carling, D., and Hardie, D.G. (1996). Characterization of the AMP-activated protein kinase kinase from rat liver and identification of threonine 172 as the major site at which it phosphorylates AMP-activated protein kinase. J. Biol. Chem. *271*, 27879–27887.

Horne, J.A., and Ostberg, O. (1976). A self-assessment questionnaire to determine morningness-eveningness in human circadian rhythms. Int. J. Chronobiol. *4*, 97–110.

Jeon, S.M. (2016). Regulation and function of AMPK in physiology and diseases. Exp. Mol. Med. *48*, e245.

Jordan, S.D., Kriebs, A., Vaughan, M., Duglan, D., Fan, W., Henriksson, E., Huber, A.L., Papp, S.J., Nguyen, M., Afetian, M., et al. (2017). CRY1/2 selectively repress PPARδ and limit exercise capacity. Cell Metab. *26*, 243–255.e6.

Koves, T.R., Ussher, J.R., Noland, R.C., Slentz, D., Mosedale, M., Ilkayeva, O., Bain, J., Stevens, R., Dyck, J.R., Newgard, C.B., et al. (2008). Mitochondrial overload and incomplete fatty acid oxidation contribute to skeletal muscle insulin resistance. Cell Metab. *7*, 45–56.

Küüsmaa, M., Schumann, M., Sedliak, M., Kraemer, W.J., Newton, R.U., Malinen, J.P., Nyman, K., Häkkinen, A., and Häkkinen, K. (2016). Effects of morning versus evening combined strength and endurance training on physical performance, muscle hypertrophy, and serum hormone concentrations. Appl. Physiol. Nutr. Metab. *41*, 1285–1294.

Lamia, K.A., Sachdeva, U.M., DiTacchio, L., Williams, E.C., Alvarez, J.G., Egan, D.F., Vasquez, D.S., Juguilon, H., Panda, S., Shaw, R.J., et al. (2009). AMPK regulates the circadian clock by cryptochrome phosphorylation and degradation. Science *326*, 437–440.

Li, H., Handsaker, B., Wysoker, A., Fennell, T., Ruan, J., Homer, N., Marth, G., Abecasis, G., and Durbin, R.; 1000 Genome Project Data Processing Subgroup (2009). The Sequence Alignment/Map format and SAMtools. Bioinformatics *25*, 2078–2079.

Martin, D.S., Levett, D.Z., Mythen, M., and Grocott, M.P.; Caudwell Xtreme Everest Research Group (2009). Changes in skeletal muscle oxygenation during exercise measured by near-infrared spectroscopy on ascent to altitude. Crit. Care *13*, S7.

Martin, M. (2011). Cutadapt removes adapter sequences from high-throughput sequencing reads. EMBnet J. *17*, 2011.

McCarthy, J.J., Andrews, J.L., McDearmon, E.L., Campbell, K.S., Barber, B.K., Miller, B.H., Walker, J.R., Hogenesch, J.B., Takahashi, J.S., and Esser, K.A. (2007). Identification of the circadian transcriptome in adult mouse skeletal muscle. Physiol. Genomics *31*, 86–95.

Mihaylova, M.M., and Shaw, R.J. (2011). The AMPK signalling pathway coordinates cell growth, autophagy and metabolism. Nat. Cell Biol. *13*, 1016–1023.

Nangle, S.N., Rosensweig, C., Koike, N., Tei, H., Takahashi, J.S., Green, C.B., and Zheng, N. (2014). Molecular assembly of the period-cryptochrome circadian transcriptional repressor complex. Elife *3*, e03674.

Narkar, V.A., Downes, M., Yu, R.T., Embler, E., Wang, Y.X., Banayo, E., Mihaylova, M.M., Nelson, M.C., Zou, Y., Juguilon, H., et al. (2008). AMPK and PPARδ agonists are exercise mimetics. Cell *134*, 405–415.

Neufeld-Cohen, A., Robles, M.S., Aviram, R., Manella, G., Adamovich, Y., Ladeuix, B., Nir, D., Rousso-Noori, L., Kuperman, Y., Golik, M., et al. (2016). Circadian control of oscillations in mitochondrial rate-limiting enzymes and nutrient utilization by PERIOD proteins. Proc. Natl. Acad. Sci. USA *113*, E1673–E1682.

Overmyer, K.A., Evans, C.R., Qi, N.R., Minogue, C.E., Carson, J.J., Chermside-Scabbo, C.J., Koch, L.G., Britton, S.L., Pagliarini, D.J., Coon, J.J., et al. (2015). Maximal oxidative capacity during exercise is associated with skeletal muscle fuel selection and dynamic changes in mitochondrial protein acetylation. Cell Metab. *21*, 468–478.

Panda, S. (2016). Circadian physiology of metabolism. Science *354*, 1008–1015.

Partch, C.L., Green, C.B., and Takahashi, J.S. (2014). Molecular architecture of the mammalian circadian clock. Trends Cell Biol. *24*, 90–99.

Pérez-Schindler, J., Kanhere, A., Edwards, L., Allwood, J.W., Dunn, W.B., Schenk, S., and Philp, A. (2017). Exercise and high-fat feeding remodel transcript-metabolite interactive networks in mouse skeletal muscle. Sci. Rep. *7*, 13485.

Perrin, L., Loizides-Mangold, U., Chanon, S., Gobet, C., Hulo, N., Isenegger, L., Weger, B.D., Migliavacca, E., Charpagne, A., Betts, J.A., et al. (2018). Transcriptomic analyses reveal rhythmic and CLOCK-driven pathways in human skeletal muscle. Elife *7*.

Reilly, T., and Waterhouse, J. (2009). Sports performance: is there evidence that the body clock plays a role? Eur. J. Appl. Physiol. *106*, 321–332.

Reinke, H., and Asher, G. (2019). Crosstalk between metabolism and circadian clocks. Nat. Rev. Mol. Cell Biol. *20*, 227–241.

Robinson, M.D., McCarthy, D.J., and Smyth, G.K. (2010). edgeR: a Bioconductor package for differential expression analysis of digital gene expression data. Bioinformatics *26*, 139–140.

Sato, S., Basse, A.L., Schönke, M., Chen, S., Samad, M., Altintas, A., Laker, R.C., Dalbram, E., Barres, R., Baldi, P., et al. (2019). Time of exercise specifies the rewiring of muscle metabolic pathways and systemic energy homeostasis. Cell Metab. https://doi.org/10.1016/j.cmet.2019.03.013.

Sergushichev, A. (2016). An algorithm for fast preranked gene set enrichment analysis using cumulative statistic calculation. 10.1101/060012.

Shackelford, D.B., and Shaw, R.J. (2009). The LKB1-AMPK pathway: metabolism and growth control in tumour suppression. Nat. Rev. Cancer *9*, 563–575.

Starnes, J.W., Parry, T.L., O'Neal, S.K., Bain, J.R., Muehlbauer, M.J., Honcoop, A., Ilaiwy, A., Christopher, P.M., Patterson, C., and Willis, M.S. (2017). Exercise-induced alterations in skeletal muscle, heart, liver, and serum metabolome identified by non-targeted metabolomics analysis. Metabolites *7*, https://doi.org/10.3390/metabo7030040.

Thosar, S.S., Herzig, M.X., Roberts, S.A., Berman, A.M., Clemons, N.A., McHill, A.W., Bowles, N.P., Morimoto, M., Butler, M.P., Emens, J.S., et al. (2018). Lowest perceived exertion in the late morning due to effects of the endogenous circadian system. Br. J. Sports Med. *52*, 1011–1012.

Weinert, D., and Waterhouse, J. (2007). The circadian rhythm of core temperature: effects of physical activity and aging. Physiol. Behav. *90*, 246–256.

Zhang, R., Lahens, N.F., Ballance, H.I., Hughes, M.E., and Hogenesch, J.B. (2014). A circadian gene expression atlas in mammals: implications for biology and medicine. Proc. Natl. Acad. Sci. USA *111*, 16219–16224.

Zheng, B., Albrecht, U., Kaasik, K., Sage, M., Lu, W., Vaishnav, S., Li, Q., Sun, Z.S., Eichele, G., Bradley, A., et al. (2001). Nonredundant roles of the mPer1 and mPer2 genes in the mammalian circadian clock. Cell *105*, 683–694.

STAR★METHODS

KEY RESOURCES TABLE

REAGENT or RESOURCE	SOURCE	IDENTIFIER
Antibodies		
Rabbit mAb Phospho-AMPKα (Thr172)	Cell Signaling Technology	mAb #2535; RRID: AB_331250
Rabbit mAb AMPKα	Cell Signaling Technology	mAb #6707; RRID: AB_10698749
Rabbit mAb LKB1	Cell Signaling Technology	D60C5, #3047; RRID: AB_2198327
Rabbit mAb Phospho-LKB1 (Ser428)	Cell Signaling Technology	#3482; RRID: AB_2198321
Mouse mAb α-Tubulin	Sigma-Aldrich	T9026; RRID: AB_477593
Chemicals, Peptides, and Recombinant Proteins		
TRI reagent	Sigma-Aldrich	93289
LightCycler 480 Syber Green I Master	Roche	04 707 516 001
LightCycler 480 Probe Master	Roche	04 707 494 001
Critical Commercial Assays		
Glucometer	Abbott Freestyle Lite	N/A
qScript cDNA synthesis kit	Quantabio	95047
Deposited Data		
RNA-seq	Gene Expression omnibus database (GEO)	GEO: GSE117161
Metabolomics	MetaboLights	MetaboLights: MTBLS145
Experimental Models: Organisms/Strains		
Wild Type C57BL/6, 3 months old males	Envigo	N/A
Per 1/2 $^{-/-}$, 3 months old males	Zheng et al., 2001	N/A
Human male subjects, mean age 32.7 ± 11.3	Detailed in Table S7	N/A
Primers for RT qPCR	Detailed in Table S6	N/A
Software and Algorithms		
R 3.5.0	CRAN	N/A
Rdavidwebservice 1.20.0	Bioconductor (Fresno and Fernández, 2013)	N/A
EdgeR 3.24.3	Bioconductor (Robinson et al., 2010)	N/A
FGSEA 1.8.0	Bioconductor(Sergushichev, 2016)	N/A
Cutadapt v1.18	(Martin, 2011)	N/A
HTseq 0.11.1	(Anders et al., 2015)	N/A
STAR 2.6	(Dobin et al., 2013)	N/A
Samtools 1.9	(Li et al., 2009)	N/A
Other		
Regular chow	Envigo	2018 Teklad
Phenomaster metabolic cages	TSE Systems	N/A

CONTACT FOR REAGENT AND RESOURCE SHARING

Further information and requests for resources and reagents should be directed to and will be fulfilled by the Lead Contact, Gad Asher (gad.asher@weizmann.ac.il).

EXPERIMENTAL MODEL AND SUBJECT DETAILS

Animals

All animal experiments and procedures were conducted in conformity with the Weizmann Institute Animal Care and Use Committee (IACUC) guidelines. We used three months old males C57BL/6 wild type (Envigo), and *Per1/2*$^{-/-}$ (Zheng et al., 2001) back crossed to C57BL/6. All mice were housed in an SPF animal facility, at ambient temperature of ~22^{0}C, under a 12 h light-dark regimen and fed

ad libitum. ZT0 corresponds to the time lights were turned ON and ZT12 to the time lights were turned OFF in the animal facility. Mice were randomly assigned to experimental groups.

Human Subjects - Exclusion and Inclusion Criteria

Twelve healthy males (age 32.7 ± 11.3 years, height 179.7 ± 4.1 cm, body mass index 22.2 ± 1.6 $kg \cdot m^{-2}$, 2-6 hours of exercise training per week, were recruited for the human study (anthropometric parameters are detailed in Table S7). All participants had an initial medical consultation to verify they had no contraindication for exercise testing, no cardiorespiratory, metabolic or neurological diseases. To determine their chrono-type and individual phase of circadian entrainment (morning vs evening type), each subject answered the Horn and Ostberg questionnaire (Horne and Ostberg, 1976). All subjects were either moderately morning or evening type persons. The study was performed according to the Declaration of Helsinki and was approved by the local ethics committee (CPP Grenoble, Sud Est V).

METHOD DETAILS

Mouse Exercise Protocols

Exercise capacity was determined using a treadmill (Panlab Harvard Apparatus, Barcelona, Spain) running tests as detailed below and previously described (Fan et al., 2017). High-intensity test: sedentary mice, with no prior adaptation, ran on the treadmill, at 8 cm/s for 5 min followed by incrementing speed of 2 cm/s every min until they reached a pre-defined exhaustion criterion (i.e. 15 shocks / 60 sec or 20 shocks / 90 sec or 25 shocks / 120 sec). For the Moderate and Low-intensity protocols sedentary mice were acclimated to the treadmill a day prior to the test (10 min of an incrementing speed from 8 to 16 cm/s followed by 5 min at 16 cm/s). The Moderate-intensity protocol consisted of 10 min run at gradual increment of the speed from 8 to 22 cm/s, followed by constant speed of 22 cm/s. The Low intensity protocol consisted of 5 min run at 8 cm/s followed by an incrementing speed from 8 to 18 cm/s over 4 min and then constant speed of 18 cm/s. The predefined elimination criterion was blood glucose levels below 70 mg/dL. Blood glucose levels were measured using a glucometer (Abbott Freestyle Lite). All treadmill experiments were done with 0% slope, using 0.4 mA shock intensity.

Animals Activity and Food Consumption Measurements

Mice spontaneous locomotor activity and food consumption were simultaneously monitored for individually housed mice using the Phenomaster metabolic cages (TSE System). Before each experiment animals were trained for several days in the metabolic cages to enable them to properly adjust to the new housing conditions. A period of 7 days acclimatization was taken before the actual recordings. Data was collected at 15 min. All animals presented were recorded together side by side to allow adequate comparisons. The light schedule in the metabolic cages was maintained as in the animals' home cages. We reanalyzed metabolic cage data that were previously collected in our lab (Adamovich et al., 2019).

Sample Preparation for RNA-seq, Metabolomics, and Protein Analyses

Exercised mice were sacrificed 1 h from the beginning of the exercise test alongside non-exercised (control) mice. The entire gastrocnemius muscle was dissected and immediately frozen in liquid nitrogen for subsequent analyses as detailed below.

RNA Preparation for RNA-seq and Real-Time PCR Analysis

Gastrocnemius tissue samples were thawed in 2 ml TRI-reagent (Sigma, T9424). Tissue was homogenized using disperser (IKA-T18), transferred to 1.7 ml tubes and kept at room temperature for 5 min, subsequently 200 μL chloroform was added. Samples were centrifuged for 15 min at 13,000 rpm at 4°c and the supernatant was transferred to tubes containing 500 μL Isopropanol, mixed and kept at room temperature for 15 min, then centrifuged at 13,000 RPM at 4°c. The supernatant was removed and the pellet was briefly vortexed and washed twice with 1 ml of 75% cold EtOH. Finally, the pellet was dried, and dissolved in 150 μL Ultra Pure Water DNase and RNase-free (Biological Industries LTD). RNA concentration was determined using NanoDrop 2000 Spectrophotometer (Thermo Fisher Scientific). RNA libraries were prepared according to the manufacturer's protocol without further modifications, using the TruSeq Stranded mRNA Sample Preparation kit (Illumina, San Diego, CA).

RNA-seq Data Processing and Analysis

The RNA-seq data included an average sequencing depth of 20 million reads (detailed in Table S2A). Cutadapt (Martin, 2011) was used to trim low quality reads and adapter sequences. Reads were mapped using STAR (Dobin et al., 2013) to mouse genome build mm10. The BAM file was converted to SAM format using Samtools (Li et al., 2009). Read counts per gene were calculated using HTSeq-count (Anders et al., 2015) and Refseq GRCm38 gtf file. EdgeR (Robinson et al., 2010) was used for normalization and to detect differentially expressed genes after filtering based on expression levels (sum normalized counts in all samples greater than 10). Transcriptome profiling are available at Gene Expression omnibus database (GEO) with the identifier GEO: GSE117161 and the quantification is provided in Table S2B.

Several comparisons between the conditions (time and/or exercise) were made in order to detect differentially expressed genes (selected by FDR<=0.05 and absolute $\log_2$ ratio>=0.5, EdgeR exact test, n=3). Differentially expressed genes were further analyzed with RDavidWebservice (Fresno and Fernández, 2013) to detect enriched KEGG pathways. Statistical analysis and visualizations

were made using R statistical programming language. The full statistical analysis table is available in Table S2C and the downstream pathway analysis in Tables S2E and S2G.

Real-Time PCR Analysis

Real-time PCR measurements were performed using SYBR green or Taqman probes with LightCycler II machine (Roche) and normalized to the geometrical mean of three housekeeping genes: *Hprt*, *Rplp0*, *Tbp*. Primers and probes (Sigma) are listed in Table S6.

Protein Extraction, Gel Electrophoresis and Immunoblotting

The Gastrocnemius samples were thawed and total protein extraction was performed by grinding the samples in 500 μl of RIPA (50 mM Tris-HCl (pH 8), 150 mM NaCl, 1% NP-40, 0.5% sodium deoxycholate, 0.1% Sodium dodecyl sulfate) supplemented with protease and phosphatase inhibitors (1/100 Protease Inhibitor Cocktail (P8340, Sigma), 0.5 mM DTT, 100 uM NaF, 100 uM Na_2VO_4, 0.5 mM Phenylmethylsulfonyl fluoride (Sigma), followed by 30 min on ice and centrifugation at 14,800 rpm for 20 min. The supernatant was transferred, protein concentration was determined by Bradford. Samples were heated at 95°C for 5 min in Laemmli sample buffer and analyzed by SDS-PAGE and immunoblot. Rabbit mAb (Cell Signaling Technology): Phospho-AMPKα (Thr172), (mAb #2535); AMPKα (mAb #6707); LKB1 (D60C5), (#3047); Phospho-LKB1 (Ser428), (#3482); and Mouse mAb (Sigma-Aldrich): Tubulin (T9026).

Metabolomics Sample Preparation, Quality Control, Data Extraction and Analysis

Frozen gastrocnemius samples were analyzed for detection and relative quantification of metabolites by Metabolon following standard procedures as previously described (Evans et al., 2009) and detailed below. Detected metabolites and their respective quantification in each sample are provided in Table S4A. In addition, the statistical analysis to assess significantly differentially accumulating metabolites was performed using ANOVA Tests and is provided in Table S4B. The metabolomics data is publicly available in the MetaboLights database under accession number MTBLS145 (MetaboLights: MTBLS145), and in Table S4.

Sample preparation: Samples were prepared using the automated MicroLab STAR system from Hamilton Company. Several recovery standards were added prior to the first step in the extraction process for QC purposes. To remove protein, dissociate small molecules bound to protein or trapped in the precipitated protein matrix, and to recover chemically diverse metabolites, proteins were precipitated with methanol under vigorous shaking for 2 min (Glen Mills GenoGrinder 2000) followed by centrifugation. The resulting extract was divided into five fractions: two for analysis by two separate reverse phase (RP)/UPLC-MS/MS methods with positive ion mode electrospray ionization (ESI), one for analysis by RP/UPLC-MS/MS with negative ion mode ESI, one for analysis by HILIC/UPLC-MS/MS with negative ion mode ESI, and one sample was reserved for backup. Samples were placed briefly on a TurboVap (Zymark) to remove the organic solvent. The sample extracts were stored overnight under nitrogen before preparation for analysis.

QA/QC: Several types of controls were analyzed in concert with the experimental samples: a pooled matrix sample generated by taking a small volume of each experimental sample served as a technical replicate throughout the data set; extracted water samples served as process blanks; and a cocktail of QC standards that were carefully chosen not to interfere with the measurement of endogenous compounds were spiked into every analyzed sample, allowed instrument performance monitoring and aided chromatographic alignment. Instrument variability was determined by calculating the median relative standard deviation (RSD) for the standards that were added to each sample prior to injection into the mass spectrometers. Overall process variability was determined by calculating the median RSD for all endogenous metabolites (i.e., non-instrument standards) present in 100% of the pooled matrix samples. Experimental samples were randomized across the platform run with QC samples spaced evenly among the injections.

Ultrahigh Performance Liquid Chromatography-Tandem Mass Spectroscopy (UPLC-MS/MS): All methods utilized a Waters ACQUITY ultra-performance liquid chromatography (UPLC) and a Thermo Scientific Q-Exactive high resolution/accurate mass spectrometer interfaced with a heated electrospray ionization (HESI-II) source and Orbitrap mass analyzer operated at 35,000 mass resolution. The sample extract was dried then reconstituted in solvents compatible to each of the four methods. Each reconstitution solvent contained a series of standards at fixed concentrations to ensure injection and chromatographic consistency. One aliquot was analyzed using acidic positive ion conditions, chromatographically optimized for more hydrophilic compounds. In this method, the extract was gradient eluted from a C18 column (Waters UPLC BEH C18-2.1x100 mm, 1.7 μm) using water and methanol, containing 0.05% perfluoropentanoic acid (PFPA) and 0.1% formic acid (FA). Another aliquot was also analyzed using acidic positive ion conditions; it was optimized for more hydrophobic compounds. In this method, the extract was gradient eluted from the same afore mentioned C18 column using methanol, acetonitrile, water, 0.05% PFPA and 0.01% FA and was operated at an overall higher organic content. Another aliquot was analyzed using basic negative ion optimized conditions using a separate dedicated C18 column. The basic extracts were gradient eluted from the column using methanol and water, with 6.5mM Ammonium Bicarbonate at pH 8. The fourth aliquot was analyzed via negative ionization following elution from a HILIC column (Waters UPLC BEH Amide 2.1x150 mm, 1.7 μm) using a gradient consisting of water and acetonitrile with 10mM Ammonium Formate, pH 10.8. The MS analysis alternated between MS and data-dependent MSn scans using dynamic exclusion. The scan range varied slighted between methods but covered 70-1000 m/z.

Data extraction, compound identification and quantification: Raw data was extracted, peak-identified and QC processed using Metabolon's hardware and software. Compounds were identified by comparison to library entries of purified standards or recurrent unknown entities. Metabolon maintains a library based on authenticated standards (more than 3300 commercially available purified compounds) that contains the retention time/index (RI), mass to charge ratio (m/z), and chromatographic data (including MS/MS spectral data) on all molecules present in the library. Furthermore, biochemical identifications are based on three criteria: retention index within a narrow RI window of the proposed identification, accurate mass match to the library +/- 10 ppm, and the MS/MS forward and reverse scores between the experimental data and authentic standards. The MS/MS scores are based on a comparison of the ions present in the experimental spectrum to the ions present in the library spectrum. Peaks were quantified using area-under-the-curve.

Metabolite Set Enrichment Analysis

Metabolites pathway annotations were used to create metabolite sets. The FGSEA algorithm (Sergushichev, 2016) was subsequently used to perform a metabolite set enrichment analysis. Briefly, this method allows to select from an a priori defined list of metabolites sets those which have non-random behavior in a considered comparison. Thus, the algorithm identifies pathways that contain many co-regulated metabolites but with small individual effects. The normalized enrichment score (NES) and other statistics (p-values, ES, FDR) for specific comparisons (Early versus Late, control versus exercise) are reported in Tables S4D and S4F.

Human Exercise Protocols

Human subjects were evaluated on four occasions for their submaximal aerobic capacity exercise response. They performed a 1-hour submaximal constant-load exercise test, which corresponds to 50% of their maximal power output (maximal power output trial: 5 min at 100 Watt, next 5 min at 150 Watt followed by gradual increase in exercise load until exhaustion). The test was performed on two occasions, at two different times of the day in a balance randomized order, at 08:00 am and at 06:00 pm. Each session was separated by a minimum interval of 2.5 days. Subjects refrained from physical activity the day before and the day of the test, slept for at least 7h the night before the tests, abstained from drinking caffeinated beverages and alcohol on test days, and had a standardized meal 2 h prior to the tests (500-600 Kcal, 50% carbohydrates / 20% lipids / 30% proteins). Before the first session each subject was measured and weighed and then was installed on the ergocycle for saddle and handlebar adjustments. Those settings were reproduced for the two tests. The individual target pedaling frequency was determined before the first test and had to remain constant within a range of ± 5 rpm throughout all tests. The room temperature was standardized at 21°C for all tests.

Measurements and Statistical Analysis of Human Exercise Performance

The subject was carefully installed on a computer-controlled electrically-braked cycle ergometer (Ergometrics 800, Ergoline, Bitz, Germany). The submaximal constant-load exercise test was performed at 50% of the individual maximal power output and lasted 1 h. Breath-by-breath minute ventilation, gas exchanges and heart rate were measured continuously (Medisoft, Dinant, Belgium). Glycemia (Xpress2, Nova Biomedical UK, Runcorn, UK) and lactatemia (Lactate Plus, Nova biomedical Corporation, Waltham, MA) from a finger capillary blood sample, intra-auricular temperature (Thermoscan, Braun, Lausanne, Switzerland), and rate of perceived exertion (on a 10-cm Visual Analogue Scale) were measured after 5 min of rest, after 5 min cycling at 100W, 5 min cycling at 150W, at exhaustion for the maximal incremental test and at 15, 30, 45 and 60 min of the submaximal constant-load cycling test.

The time of day effect on rest measurements (Time 0) was analyzed by t-test. The effect of exercise and time of day (Early vs. Late) was analyzed by a two-way repeated measures ANOVA. Post-hoc Tukey's tests were applied to determine a difference between two mean values if the ANOVA revealed a significant main effect or interaction effect. For all statistical analyses, a two-tailed alpha level of 0.05 was used as the cut-off for significance.

QUANTIFICATION AND STATISTICAL ANALYSIS

Detailed descriptions of sample size and statistical methods for computation can be found in Figure Legends. The sample sizes were based on those commonly used in the field without predetermination by statistical methods. All samples/ animals that met proper experimental conditions were included in the analyses. In general, ANOVA analyses were used for datasets with more than two groups and Student's t tests were used for datasets with only two groups. Statistics were calculated in either Microsoft Excel (t tests) or R (ANOVA and Tuckey's post-hoc tests).

DATA AND SOFTWARE AVAILABILITY

The transcriptome profiling has been deposited in the Gene Expression omnibus database (GEO) under GEO: GSE117161.

The metabolomics data have been deposited in the MetaboLights database under accession number MetaboLights: MTBLS145.